

## CHAPTER 7

### Tolfa, Cerveteri and Manziana volcanic area

GIAMPIERO POLI<sup>1</sup>\* and DIEGO PERUGINI<sup>1</sup>

<sup>1</sup> Department of Earth Sciences, University of Perugia, Piazza Università, 06100, Perugia, Italy

#### 7.1 HISTORICAL PERSPECTIVE

A few kilometres from Civitavecchia, there is Tolfa Mountains territory formed by a hilly mass that rises for 638 meters and is characterized by variable morphology. The scenery is moved by numerous ranges mostly covered with coppice or extensive grazing land. The towns of Tolfa and Allumiere are situated on the top of these ranges which formed following a series of volcanic eruptions in the Pliocene period. This geological scenery, have for years been the treasure of these territories. Just think that Allumiere owes its origins and its name to alum, a mineral of world-wide interest during past centuries.

The territory of Tolfa has been involved in human settlements ever since back in the Neolithic age; findings date back to that era, as well as to the bronze age, the iron age, and the ProtoVillanova and Villanova age. There is a marked presence of Etruscans, as evidenced by the numerous necropolis and Etruscan tombs found in numerous locations. These attest to the presence of various inhabited centers that were located, most probably, on tuff highlands. The Etruscan civilization was ousted by the Roman civilization which also left many traces. The most thriving period for Tolfa area was

next the higher Middle Ages. The inhabited area of Tolfa extended from the Rocca towards a much wider and definite boundary with the construction of churches with squares and all the facilities required for daily social life and expanding for the most part after the discovery of alum (1460-1462) by Giovanni da Castro.

On the origins of the name «Tolfa» there are two possibilities: the name could derive from the root «TUL», of Etruscan origin, which meant «to raise» and therefore could indicate the altitude referred to its geographical location; or it could originate from the Lombard culture, present in that area from the end of the VI century, in whose onomatopoeically the end sound of «ULFO» is frequently used.

#### 7.2 GEOLOGICAL SETTING

The southernmost outcrop of the Tuscan Magmatic Province is constituted by a suite of volcanic rocks cropping out in the Tolfa, Cerveteri and Manziana areas (Fig. 1; TCMV), about 100 km north of Rome.

Formations belonging to the Tuscan nappe constitute the Tolfa hills; Liassic limestones and the Upper Cretaceous-Oligocene shaley formations are overlaid by a complex of flysch formations that can be correlated with the

\* Corresponding author, E-mail: [polig@unipg.it](mailto:polig@unipg.it)

Ligurid Units which crop out in southern Tuscany, according to structural maps of the Northern Apennines (Boccaletti and Coli, 1982).

The three main outcrops are located at Tolfa, Cerveteri and Manziana, whereas smaller outcrops are present at Tolfaccia, Roccaccia and Montagnola. The volcanic rocks occur as a series of lava domes, often fumarolized and silicified, bearing variable amounts of magmatic enclaves, and forming a NW-SE trending uplifted structure. An explosive volcanic activity, leading to the formation of ignimbritic deposits, now eroded or intensely altered,

preceded the emplacement of the lava domes. Age of the Tolfa volcanic rocks is 4.2-2.3 Ma, according to Ferrara *et al.* (1988) and Fornaseri (1985). Clausen and Holm (1990) reported more variable and younger ages with three main stages: 3.7-3.8 Ma, 2.3-2.5 Ma, and 1.8 Ma.

Although TCMV rocks have been traditionally considered typical anatectic magmas, recent hypothesis (Peccerillo *et al.*, 1987; Clausen and Holm, 1990; Pinarelli, 1991; Bertagnini *et al.*, 1995) suggest that this magmatism may be related to the rise of mafic alkaline magmas derived from partial melting of a mantle enriched in incompatible elements.

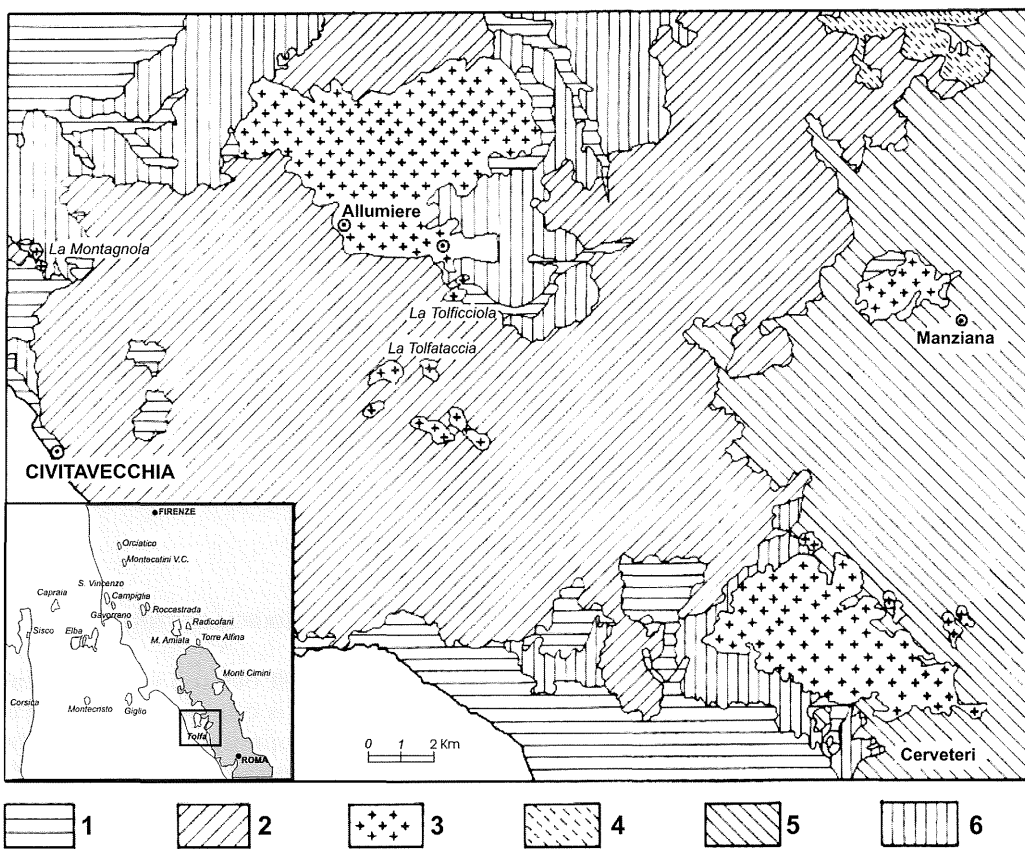


Fig. 1 – Schematic geological map of the Tolfa area: 1 = Pietraforte Unit; 2 = «Flysch Tolfetani» series; 3 = Tolfa-Cerveteri-Manziana volcanics; 4 = Vico Volcano; 5 = Sabatini volcanics; 6 = Neogene deposits. Modified from Pinarelli (1991).

The rise of these magmas may have generated crustal anatexis melts which interacting in variable amount with the mafic magmas to produce partially hybridized rocks.

### 7.3 PETROGRAPHY

Modal analyses of the volcanic rocks and enclaves are given in Table 1 (Pinarelli, 1991). Note, however, that a confident estimate of the modal proportion of minerals in each sample is difficult to achieve because of the presence of a glassy groundmass in the rocks, and of the large size of phenocrysts (1.0-5.0 mm). A chemical classification (TAS, Fig. 2A) is preferred and TMCV rocks can be divided into two groups: (i) trachydacites and (ii) rhyolites. Mafic enclaves (basaltic trachy-andesite and trachy-andesite in composition) have been found in the both groups, but are lacking in the most silicic rhyolites. The two groups of rocks crop out in different areas and can be related to the three stages of outpouring: trachydacites in Tolfa and Cerveteri at 3.7-3.8 Ma and 2.3-2.5 Ma; rhyolites in Manziana at 2.3-2.5 Ma and 1.8 Ma; high-silica rhyolites in Manziana at 1.8 Ma.

#### *Trachydacites*

Most of the samples contain up to centimetric magmatic enclaves and microscopic metasedimentary enclaves consisting of holocrystalline rocks constituted by xenomorphic quartz and biotite. Groundmass (50-79%) is perlitic, fluidal or microcrystalline containing phenocrysts of plagioclase, sanidine, ortho- and clinopyroxene, and biotite sometimes fractured. Accessory minerals are zircon, apatite and titanomagnetite. Plagioclase, often euhedral, has a labradoritic compositions ( $An_{49-60}$ ), with normal zoning, and typically shows resorption textures. Sanidine is euhedral, corroded, and contains inclusions of orthopyroxene, plagioclase, biotite, accessory minerals, and titanomagnetite. Orthopyroxene is euhedral, sometimes altered to chlorite or calcite; rare

augitic clinopyroxene can also be found. Biotite is euhedral, sometimes deformed and rarely chloritized. Plagioclase often forms clusters with orthopyroxene, where it has the same composition as in the individual grains. Aggregates of orthopyroxene, biotite, and accessory minerals are also commonly present.

#### *Rhyolites*

Most of the samples contain up to centimetric magmatic enclaves and microscopic metasedimentary quartz-biotite-rich enclaves. Groundmass (60-72%) is holocrystalline containing microlites of pyroxene and feldspars, and phenocrysts of normal and reverse-zoned plagioclase ( $An_{35-70}$ ), sometimes mantled by sanidine, highly fractured sanidine with inclusions of biotite, very rare and fairly fresh biotite, corroded quartz with wide embayment, and strongly altered orthopyroxene.

Groundmasses from the two occurrence of the most silicic rhyolites are different but contain almost the same phenocrysts: euhedral, corroded sanidine, slightly zoned plagioclase ( $An_{20-26}$ ), quartz, and biotite. Groundmass from Montagnola (80%) is micro-crystalline, whereas that from Cerveteri (69%) is glassy and do not contain quartz. No enclaves both metasedimentary and magmatic have been found.

#### *Mafic enclaves*

On the K-SiO<sub>2</sub> diagram (Peccerillo and Taylor, 1976; Fig. 2B) enclaves can be divided into two main groups having different affinity: high-potassium and shoshonitic. They display a rounded shape, crenulated margins and shaded contacts with the host rocks. Commonly, xenocrysts deriving from the host magma are observed within enclaves, indicating a molten state of enclaves when they came in contact with the host magma. Mineral chemistry and detailed petrography can be found in Bertagnini *et al.* (1995).

The first group (shoshonitic enclaves) is found in Manziana rock types. These enclaves

TABLE 1  
*Mineralogical modal compositions of volcanic rocks and enclaves from the TMCV.  
 Rocc.=Roccaccia; Cerv.=Cerveteri; Mont.=Montagnola. (after Pinarelli, 1991).*

| Mineral      | Enclaves       |       |             |       | Trackydacites |       |           |       | Rhyolites |       |       |       |       |
|--------------|----------------|-------|-------------|-------|---------------|-------|-----------|-------|-----------|-------|-------|-------|-------|
|              | High-potassium |       | Shoshonitic |       | Tolfa         |       | Cerveteri |       | Manziana  |       | Rocc. | Cerv. | Mont. |
|              | Min            | Max   | Min         | Max   | Min           | Max   | Min       | Max   | Min       | Max   |       |       |       |
| Plagioclase  | 7.27           | 4.21  | 32.88       | 17.12 | 20.36         | 22.77 | 10.03     | 17.27 | 7.00      | 14.17 | 23.16 | 8.41  | 2.00  |
| Sanidine     | 0.00           | 22.62 | 31.39       | 25.30 | 14.79         | 14.50 | 7.90      | 13.06 | 19.15     | 14.61 | 11.01 | 15.42 | 8.19  |
| Biotite      | -              | -     | 19.19       | 24.39 | 4.02          | 4.22  | 2.13      | 4.14  | 1.72      | 2.83  | 4.94  | 7.51  | 1.50  |
| Pyroxene     | 2.28           | 3.43  | 12.94       | 16.36 | 1.66          | 7.76  | 3.80      | 7.71  | 0.00      | 1.33  | 5.44  | 0.00  | 0.00  |
| Quartz       | -              | -     | -           | -     | 0.00          | 0.00  | 0.00      | 0.00  | 3.10      | 3.72  | 0.00  | 0.00  | 8.49  |
| Accessories* | -              | 3.20  | 3.57        | 3.11  | 0.47          | 1.85  | 0.61      | 1.14  | 0.00      | 0.00  | 0.51  | 0.10  | 0.00  |
| Groundmass   | 90.44          | 66.53 | 0.00        | 13.71 | 58.70         | 48.90 | 75.52     | 56.61 | 69.04     | 63.33 | 54.94 | 68.57 | 79.82 |

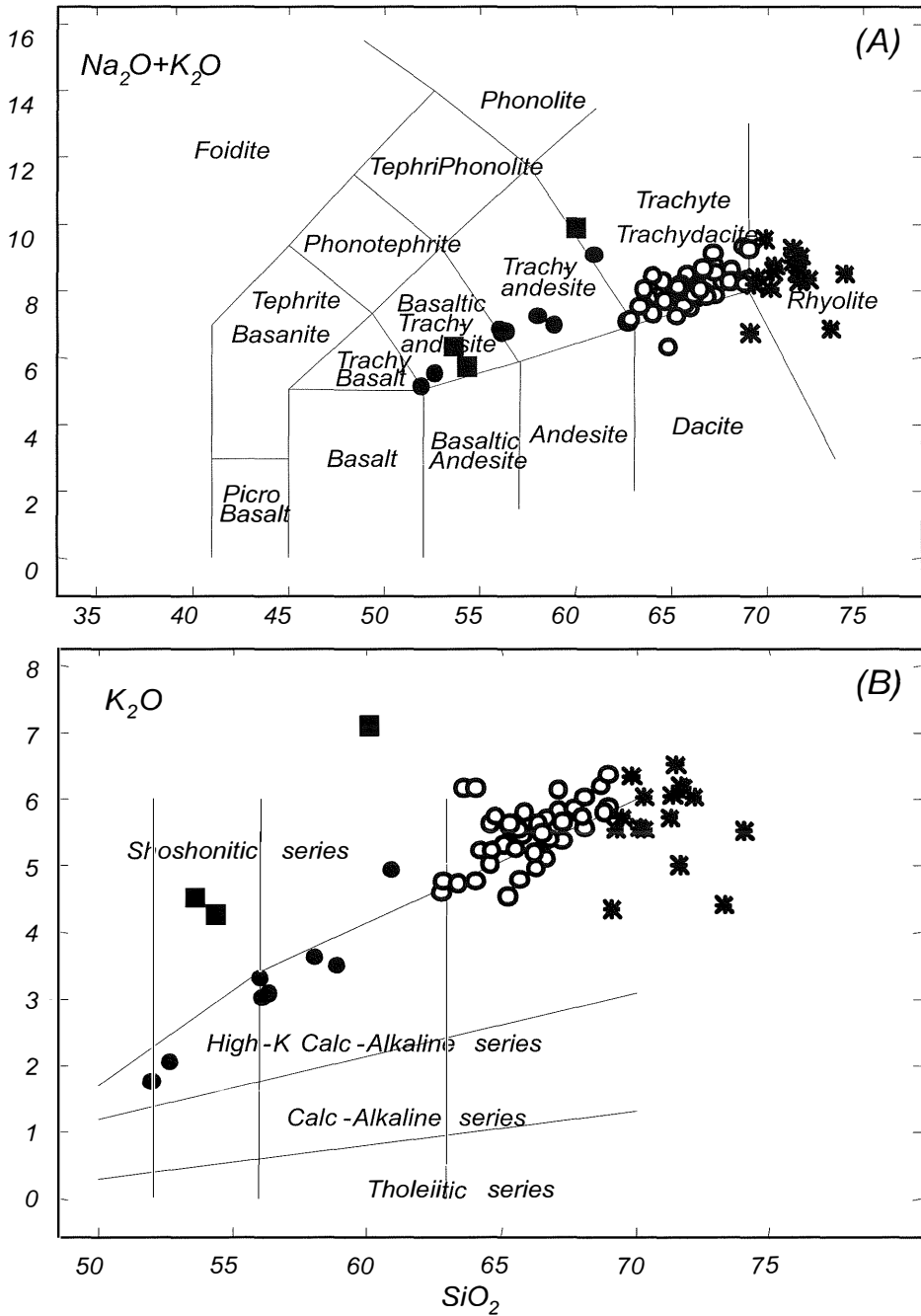


Fig. 2 – TAS classification diagram (Le Bas *et al.*, 1986) (A), and K<sub>2</sub>O vs. SiO<sub>2</sub> diagram (Peccerillo and Taylor, 1976) (B) for TCM volcanic rocks and magmatic inclusions (A). Squares: shoshonitic enclaves; circles: high-potassium enclaves; open circles: trachydacite; stars: rhyolites.

are subspherical, and range from <1.0 mm to 10 cm in diameter. They have mainly a microgranular holocrystalline texture with rare interstitial glass, and consist of acicular biotite and zoned labradoritic plagioclase ( $An_{55-70}$ ) that is sometimes mantled by K-feldspar, with salitic to augitic clinopyroxene and ellipsoidal resorbed orthopyroxene. K-feldspar and titanomagnetite are also present in small amounts.

The second type of enclave (high-potassium), found in all rocks, reaches sizes up to 30-40 cm in diameter. These enclaves exhibit a scoriaceous texture due to the presence of vesicles that can reach 4.0-5.0 mm. The microlitic groundmass is composed of acicular plagioclase ( $An_{24-67}$ )  $\pm$  K-feldspar  $\pm$  clinopyroxene, and contains normal- and inverse-zoned plagioclase ( $An_{26-81}$ ), K-feldspar, hyperstene to augitic clinopyroxene, and quartz, all of which exhibit wide corrosion embayment and reaction rims. In some cases evidence of interaction with the shoshonitic enclaves are found.

#### 7.4 GEOCHEMISTRY

Whole rock major and trace element compositions have been analysed by Clausen and Holm (1990), Pinarelli (1991), De Rita *et al.* (1994), Bertagnini *et al.* (1995), and De Rita *et al.* (1997), and Table 2 reports selected analyses. TMCV rocks have up to 2.6% (trachydacites) and up to 4% (rhyolites) of normative corundum, and a peraluminous index in the range 1.0-1.5 with rhyolites having the highest values. Figure 3 shows representative Harker diagrams for the volcanic rocks and enclaves.  $Al_2O_3$ ,  $FeO_{tot}$  and CaO decrease regularly with increasing silica content from mafic enclaves to rhyolites. In figure 2B all the samples plot on the line dividing HK and shoshonitic series. The two groups of enclaves can be easily recognized on the basis of the trace element diagrams (Fig. 4), because shoshonitic enclaves have, in average, higher amounts of all the LILE, especially Sr

and Ba with respect to the high-potassium enclaves: Rb (273 vs. 197 ppm), Sr (650 vs. 300 ppm), Ba (1100 vs. 475 ppm), Pb (70 vs. 40 ppm) and Th (38 vs. 23 ppm). Trachydacites show minor variations when plotted against  $SiO_2$ , whereas rhyolites show a decrease in Sr, Ba, LREE, and Zr contents, and an increase in the concentration of Rb with increasing  $SiO_2$ .

The initial Sr isotope ratios (ages as reported by Clausen and Holm, 1996) of the trachydacites and rhyolites range from 0.71285 to 0.71388, and from 0.71227 to 0.71441, respectively. Among studied rocks high-potassium enclaves have the lowest initial Sr isotope ratios (0.70791-0.70962), whereas shoshonitic enclaves (0.71173-0.7127) have ratios intermediate between those of high-potassium enclaves and the trachydacites.

The lead isotope ratios of the volcanic rocks and enclaves are quite variable. No differences exist between the two groups of enclaves that show the most radiogenic values (e.g. 208/204 = 38.874-39.025). The same holds for the most felsic rocks, even if trachydacites have higher range of values with respect to rhyolites (38.79-38.914 versus 38.859-38.895). As a whole, all the samples exhibit typical crustal lead isotope compositions.

#### 7.5 PETROGENESIS

The differences in initial Sr and Pb isotope compositions of mafic enclaves and their host rocks, as well as the lack of continuous trends connecting the volcanic rocks and enclaves on the major- and trace-element variation diagrams, rule out the possibility that the volcanic rocks were derived from a mafic parental magma, represented by the enclaves, through closed system differentiation. Moreover, some data, such as the crustal isotopic signatures, the high alumina contents, and the presence of metasedimentary enclaves, suggest that a crustal anatectic magma may have played a key role for the genesis and evolution of the TCMV rocks. In addition subspherical shapes, convoluted contacts with the

host rocks, fluidal textures, and presence of glass and vesicles of enclaves indicate that they have been incorporated in a molten state. However, the presence of large corroded and embayed xenocrysts of quartz and feldspar, belonging to the host magma and now occurring within enclaves suggests that enclaves do not represent primary magmas, but interacted to variable extents with the felsic host magmas. An interaction process between felsic magma(s) and mafic magma(s) is, hence, the most viable on the basis of petrography and geochemistry, and enclaves can be considered hybrid products of a mixing process involving primary mafic magmas and anatectic liquids represented by the rhyolites (Poli and Tommasini, 1991). However this process does not explain the two type of enclaves that cannot derive one from the other by evolution processes such as crystal fractionation or mixing plus crystal fractionation owing to large geochemical differences. Crude calculations give absurd results mainly for LILE and REE elements. Therefore, two types of mantle derived magmas should be hypothesized as mafic end-members for the mixing process. The felsic end-member can be envisaged as the most felsic rhyolites. Compositional characteristics of some rhyolites such as the strong depletion in elements stored in feldspar Eu, Sr, Ba (e.g. 30 ppm of Sr, 40 ppm of Ba, and Eu anomaly 0.12) and enrichment in incompatible elements (U, Th, Rb) indicate that they cannot be produced by anatectic processes because the degree of melting required to produce such low Sr and Ba contents in the liquid would be too low (less than 10%). The low isotopic differences between high-silica rhyolites and rhyolites indicate, on the contrary, that the most silicic rhyolites could derive from the rhyolites by crystal fractionation processes, able to deplete at very low values Sr and Ba by fractionation of feldspars. The other rhyolites have major and trace element compositions very similar to anatectic magma from S.Vincenzo, Roccastrada and leucocratic facies of Tuscan granitoids. They have, however, lower isotopic

ratios just corresponding to the lower values of Paleozoic garnet-bearing micaschists considered the sources of anatectic melts in the S.Vincenzo area (see Part. IV, Chap. 1). Thus, such rocks can be considered the source of the felsic rocks cropping out in the TCMV area.

Emplacement ages and the different occurrence of enclaves in the acid hosts can help to decipher genesis and evolution of TCMV rocks. A series of magma chambers containing a rhyolitic magma derived from partial melting of a crustal source similar to the less radiogenic rocks of the Paleozoic garnet-bearing micaschists were injected by a mafic magma having the geochemical characteristics of high-potassium enclaves and interaction processes between the two magmas produced mixed rocks containing enclaves represented by the trachydacitic rocks. Such magmas erupted only in the Tolfa and Cerveteri areas in two successive events at ca 3.8 and 2.4 Ma. At the younger stage rhyolitic rocks were emplaced in the Cerveteri and Manziana areas bearing, the former only high-potassium enclaves, and the latter both type of enclaves. This indicate that a slightly different magma chamber was present under the Manziana area. A second shoshonitic mantle derived magma was injected into a chamber where was present a mush constituted by felsic magmas and high-potassium mafic magmas. Note that, though these rocks contain both types of enclaves they still remain rhyolites, indicating that the felsic magma underwent very small degrees of interaction with mafic magmas. Finally at 1.8 Ma in the Manziana area only rhyolites lacking of enclaves were emplaced. Along this complex frame, possibly batches of melt present in the magma chambers fractionated to produce the high-silica rhyolitic magma.

The two different mafic magmas derived from a mantle with variable degrees of enrichment in incompatible elements and radiogenic Pb and Sr as evidenced by their geochemical characteristics. In order to decipher possible mantle sources in relation with other mafic magmas belonging to the Tuscan Magmatic Province (TMP) in figure 5

TABLE 2

|                                    | <i>TMR97</i> | <i>TMR95</i> | <i>TMR107b</i> | <i>TMR107a</i> | <i>TMR107c</i> | <i>MAN 1</i> | <i>MAN 1</i> | <i>asd2</i> | <i>asd5</i> | <i>asd8</i> | <i>asd9</i> |
|------------------------------------|--------------|--------------|----------------|----------------|----------------|--------------|--------------|-------------|-------------|-------------|-------------|
| SiO <sub>2</sub>                   | 54.37        | 60.02        | 52.64          | 58.82          | 60.91          | 51.92        | 51.92        | 56.01       | 58          | 56.29       | 56.09       |
| TiO <sub>2</sub>                   | 0.88         | 0.64         | 1.4            | 1.13           | 0.99           | 1.14         | 1.14         | 1.17        | 1.13        | 1.17        | 1.12        |
| Al <sub>2</sub> O <sub>3</sub>     | 18.82        | 18.53        | 19.34          | 17.83          | 18.04          | 17.09        | 17.09        | 16.74       | 16.24       | 16.85       | 16.58       |
| Fe <sub>2</sub> O <sub>3</sub>     | 6.87         | 2.35         | 6.88           | 5.53           | 5.32           | 6.39         | 6.39         | 3.66        | 3.08        | 3.68        | 3.14        |
| FeO                                | 1.52         | 1.46         | 1.2            | 0.86           | 0.19           | 1.84         | 1.84         | 3.03        | 3.34        | 2.89        | 3.43        |
| MnO                                | 0.1          | 0.06         | 0.05           | 0.05           | 0.04           | 0.22         | 0.22         | 0.1         | 0.09        | 0.1         | 0.09        |
| MgO                                | 2.22         | 1.27         | 2.77           | 1.48           | 0.51           | 4.7          | 4.7          | 3.19        | 2.6         | 3.11        | 3.35        |
| CaO                                | 5.69         | 4.31         | 7.5            | 5.01           | 3              | 9.62         | 9.62         | 7.99        | 6.86        | 7.86        | 8.18        |
| Na <sub>2</sub> O                  | 1.43         | 2.82         | 3.46           | 3.46           | 4.18           | 3.36         | 3.36         | 3.53        | 3.6         | 3.71        | 3.7         |
| K <sub>2</sub> O                   | 4.27         | 7.08         | 2.07           | 3.51           | 4.93           | 1.76         | 1.76         | 3.32        | 3.63        | 3.08        | 3.02        |
| P <sub>2</sub> O <sub>5</sub>      | 0.47         | 2.07         | 0.2            | 0.25           | 0.18           | 0.26         | 0.26         | 0.33        | 0.29        | 0.32        | 0.33        |
| LOI                                | 3.31         | 1.3          | 2.43           | 2              | 1.54           | 1.7          | 1.7          | 0.93        | 1.12        | 0.95        | 0.97        |
| Rb                                 | 205          | 341          | 109            | 224            | 259            | 157          | 157          | 198         | 254         | 185         | 194         |
| Sr                                 | 572          | 727          | 352            | 291            | 266            | 321          | 321          | 313         | 285         | 306         | 321         |
| Ba                                 | 1107         | 1076         | 368            | 439            | 620            | 554          | 554          | 456         | 438         | 449         | 436         |
| Th                                 | 26           | 50           | 13             | 26             | 31             | -            | -            | -           | -           | -           | -           |
| Zr                                 | 196          | 287          | 208            | 245            | 250            | 152          | 152          | 224         | 251         | 233         | 236         |
| Cr                                 | -            | -            | -              | -              | -              | 143          | 143          | 56          | 43          | 56          | 59          |
| Y                                  | 24           | 29           | 83             | 64             | 50             | 31           | 31           | 37          | 40          | 35          | 38          |
| Co                                 | -            | -            | -              | -              | -              | 30           | 30           | 21          | 20          | 21          | 21          |
| Nb                                 | 7            | 11           | 10             | 17             | 13             | -            | -            | -           | -           | -           | -           |
| La                                 | 57           | 83           | 59             | 76             | 75             | 29           | 29           | 53          | 57          | 50          | 54          |
| Ce                                 | 114          | 160          | 92             | -              | 114            | 57           | 57           | 96          | 107         | 96          | 99          |
| Nd                                 | 47           | 64           | 48             | 62             | 60             | -            | -            | -           | -           | -           | -           |
| Sm                                 | 8.2          | 11           | 10             | 12.1           | 11.5           | -            | -            | -           | -           | -           | -           |
| Eu                                 | 1.7          | 2.24         | 1.61           | 1.67           | 1.74           | -            | -            | -           | -           | -           | -           |
| Yb                                 | 1.9          | 2.8          | 6.9            | 5.5            | 4.5            | -            | -            | -           | -           | -           | -           |
| Lu                                 | 0.37         | 0.51         | 1.26           | 0.98           | 0.78           | -            | -            | -           | -           | -           | -           |
| Ni                                 | -            | -            | -              | -              | -              | 63           | 63           | 32          | 25          | 30          | 32          |
| <sup>87</sup> Sr/ <sup>86</sup> Sr | 0.71173      | 0.7127       | 0.70791        | 0.70904        | 0.70962        | -            | -            | -           | -           | -           | -           |



*Selected chemical analyses of TMCV rocks from Pinarelli (1991), De Rita et al. (1994), Bertagnini et al. (1995), and De Rita et al. (1997).*

| <i>TOLr</i> | <i>TMR111</i> | <i>TMR96</i> | <i>TMR101</i> | <i>TMR104</i> | <i>TMR94</i> | <i>TMR116</i> | <i>TMR105</i> | <i>TMR106</i> | <i>TMR92</i> | <i>TMR117</i> | <i>TMR91</i> |
|-------------|---------------|--------------|---------------|---------------|--------------|---------------|---------------|---------------|--------------|---------------|--------------|
| 53.59       | 63.34         | 64.61        | 65.72         | 66.66         | 66.65        | 64.77         | 71.29         | 71.66         | 69.13        | 74.04         | 73.36        |
| 1           | 0.74          | 0.66         | 0.62          | 0.64          | 0.62         | 0.68          | 0.37          | 0.39          | 0.53         | 0.24          | 0.13         |
| 16.9        | 16.68         | 16.45        | 15.85         | 17.11         | 16.11        | 15.2          | 15.97         | 14.5          | 13.8         | 13.31         | 12.46        |
| 5.91        | 0.65          | 2.16         | 0.95          | 1.08          | 1.2          | 0.3           | 0.31          | 2.18          | 0.72         | 0.66          | 0.77         |
| 1.82        | 3.5           | 1.65         | 2.38          | 1.2           | 1.88         | 1.86          | 0.51          | 0.25          | 0.68         | 0.88          | 0.43         |
| 0.11        | 0.06          | 0.04         | 0.05          | 0.03          | 0.04         | 0.07          | 0.01          | 0.03          | 0.06         | 0.02          | 0.03         |
| 4.87        | 1.85          | 1.4          | 1.35          | 0.75          | 1.21         | 0.94          | 0.22          | 0.31          | 1.3          | 0.25          | 0.17         |
| 6.71        | 4.26          | 3.18         | 3.5           | 2.46          | 3.11         | 3.96          | 1.04          | 1.51          | 3.04         | 1.36          | 0.78         |
| 1.8         | 2.82          | 2.47         | 2.61          | 2.86          | 2.59         | 0.6           | 3.14          | 3.28          | 2.43         | 2.97          | 2.43         |
| 4.52        | 4.74          | 5.23         | 5.45          | 5.11          | 5.38         | 5.73          | 5.71          | 4.99          | 4.34         | 5.52          | 4.4          |
| 0.45        | 0.19          | 0.12         | 0.29          | 0.11          | 0.12         | 0.11          | 0.24          | 0.03          | 0.07         | 0.03          | 0.03         |
| 2.31        | 1.1           | 1.98         | 1.17          | 1.93          | 1.05         | 1.11          | 1.13          | 0.81          | 1.83         | 0.62          | 3.99         |
| 431         | 240           | 305          | 294           | 272           | 293          | 307           | 463           | 385           | 293          | 305           | 403          |
| 765         | 244           | 264          | 256           | 240           | 56           | 70            | 90            | 91            | 250          | 119           | 29           |
| 864         | 616           | 567          | 589           | 635           | 583          | 576           | 214           | 231           | 503          | 236           | 39           |
| -           | 24            | 30           | 30            | 33            | 31           | 28            | 55            | 53            | 32           | 40            | 61           |
| 211         | 216           | 275          | 232           | 202           | 260          | 235           | 202           | 214           | 220          | 139           | 94           |
| 30          | -             | -            | -             | -             | -            | -             | -             | -             | -            | -             | -            |
| 35          | 28            | 28           | 25            | 106           | 27           | 25            | 28            | 35            | 26           | 22            | 21           |
| 24          | -             | -            | -             | -             | -            | -             | -             | -             | -            | -             | -            |
| -           | 11            | 19           | 13            | 11            | 15           | 14            | 15            | 10            | 12           | 9             | 13           |
| 76          | 55            | 51           | 61            | 61            | 52           | 54            | 56            | 71            | 51           | 57            | 50           |
| 125         | 106           | 97           | 115           | 128           | 103          | 103           | 111           | 133           | 100          | 112           | 104          |
| -           | 44            | 36           | 46            | 63            | 40           | 40            | 38            | 50            | 39           | 43            | 41           |
| -           | 8.4           | 6.7          | 8.3           | 15            | 7.4          | 7.4           | 7.1           | 9.4           | 7.3          | 7.9           | 4.6          |
| -           | 1.42          | 1.19         | 1.36          | 2.57          | 1.26         | 1.28          | 0.78          | 0.82          | 1.27         | 0.68          | 1.3          |
| -           | 2.8           | 2.4          | 2.6           | 10.1          | 2.4          | 2.3           | 2.3           | 3.4           | 2.4          | 2.7           | 2.5          |
| -           | 0.52          | 0.47         | 0.49          | 1.94          | 0.46         | 0.44          | 0.39          | 0.63          | 0.45         | 0.52          | 0.48         |
| 37          | -             | -            | -             | -             | -            | -             | -             | -             | -            | -             | -            |
| -           | 0.71373       | 0.71383      | 0.71372       | 0.71354       | 0.71371      | 0.71363       | 0.71319       | 0.71308       | 0.71374      | 0.7134        | 0.71227      |

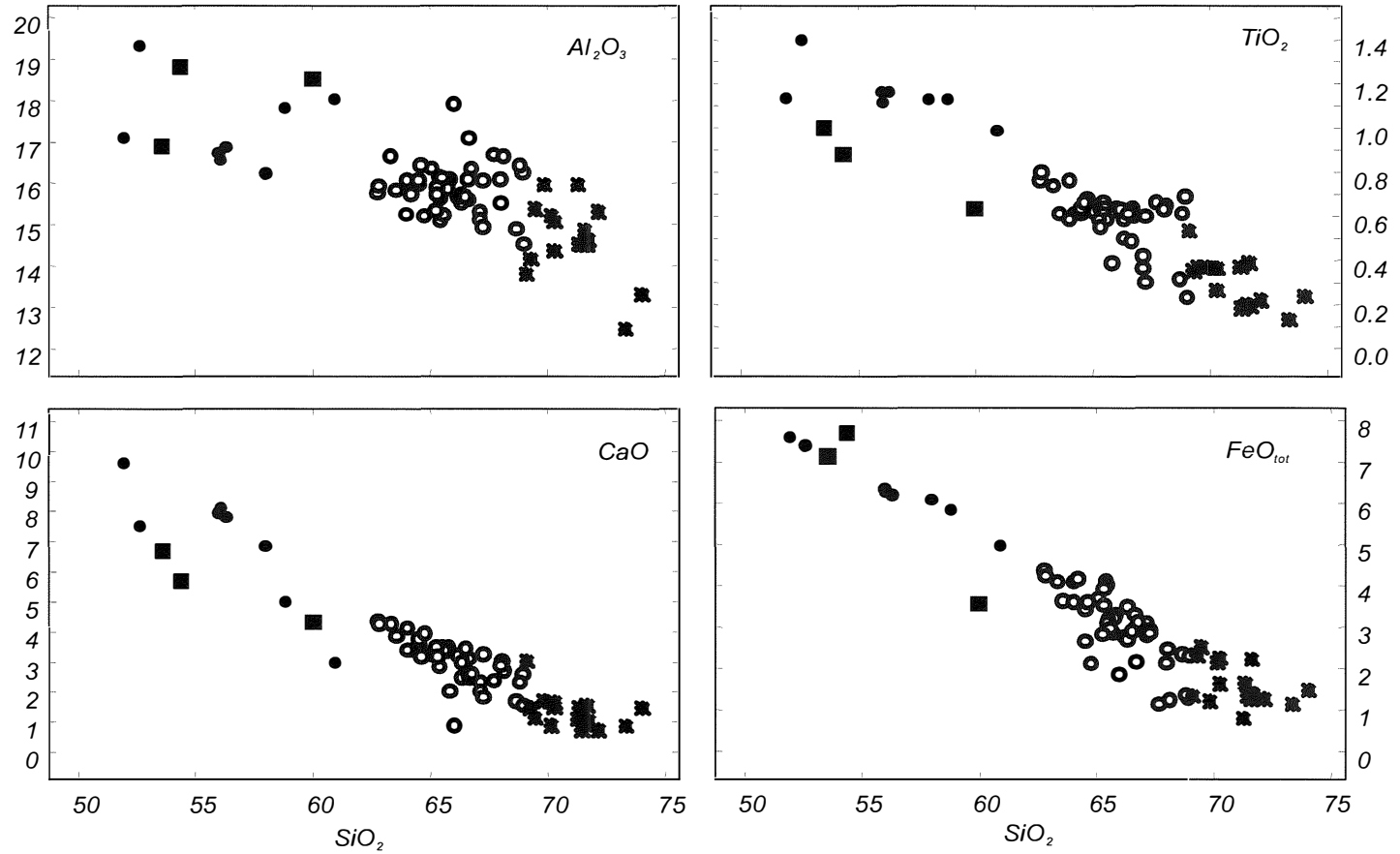


Fig. 3 – Representative major elements plotted against SiO<sub>2</sub> for Tolfa-Cerveteri-Manziana rocks. Data from Pinarelli (1991), De Rita *et al.* (1994), Bertagnini *et al.* (1995), and De Rita *et al.* (1997). Symbols as in figure 2 caption.

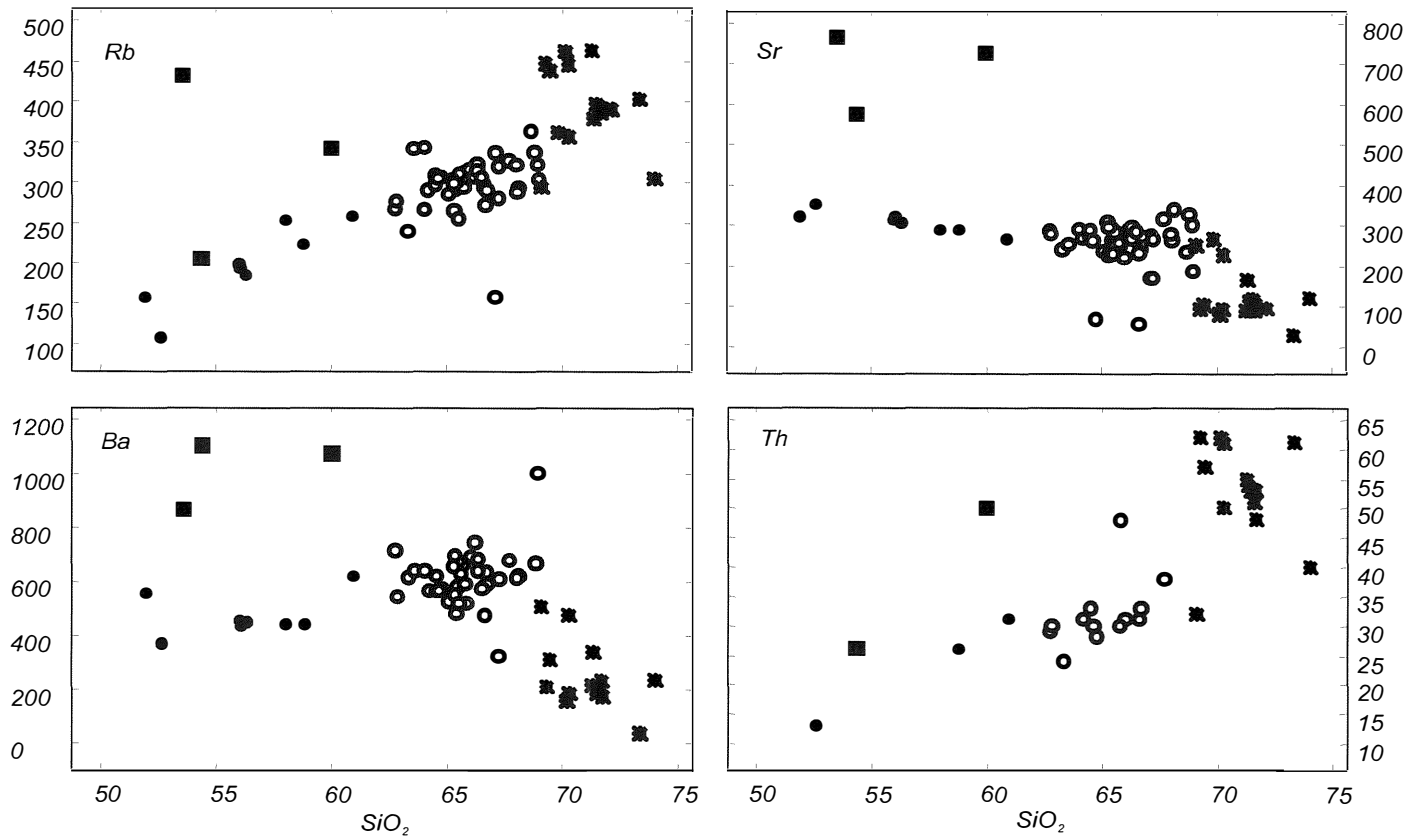


Fig. 4 – Representative trace elements plotted against  $\text{SiO}_2$  for Tolfa-Cerveteri-Manziana rocks. Data and symbols as in figure 2 caption.

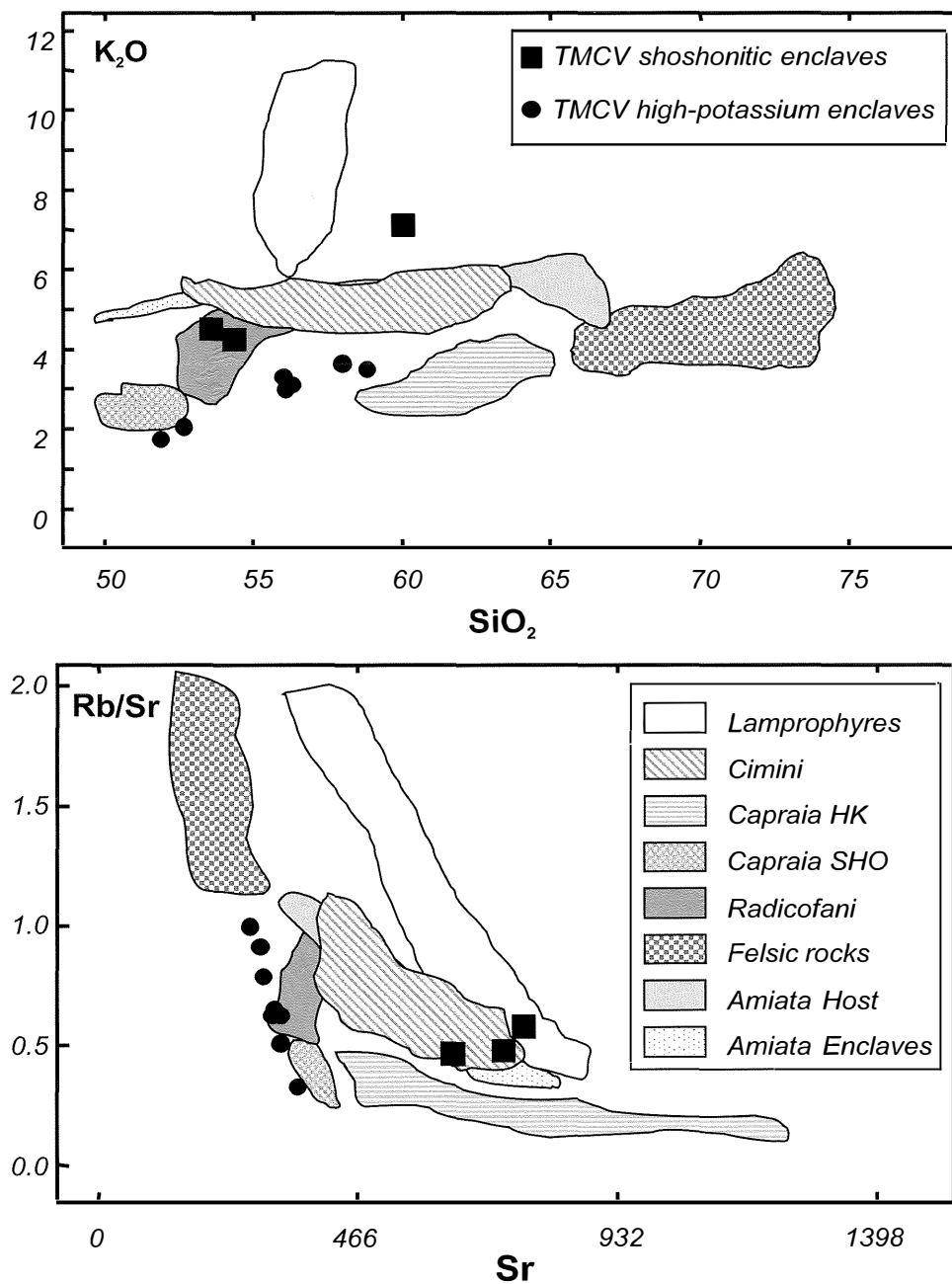


Fig. 5 –  $SiO_2$  vs.  $K_2O$  and  $Sr$  vs.  $Rb/Sr$  for volcanites and plutonites of Tuscan Magmatic Province reported with enclaves from TMC volcanic area.

SiO<sub>2</sub> vs K<sub>2</sub>O and Sr vs. Rb/Sr diagrams are reported. It is shown that high-potassium enclaves plot along the trend connecting Capraia rocks both shoshonitic and high-potassium and felsic magmas of the TMP. Shoshonitic enclaves plot, on the contrary, on Cimini, Amiata, Radicofani fields indicating an affinity with the lamproitic rocks of TMP.

